RESEARCH ARTICLE | FEBRUARY 24 2026

Impact of superlattice size on quantum efficiency and polarization in MOCVD-grown strained GaAs/GaAsP photocathodes FREE

Adam Masters ; Greg Blume ; Sushil Poudel ; Joseph Michael Grames ; Matt Poelker ; Marcy Stutzman ; Stephen Polly; Seth M. Hubbard ; Sylvain Marsillac ; Matt Grau

Appl. Phys. Lett. 128, 083501 (2026)
https://doi.org/10.1063/5.0315264
CHORUS

Applied Physics Letters ARTICLE pubs.aip.org/aip/apl

Impact of superlattice size on quantum efficiency and polarization in MOCVD-grown strained GaAs/GaAsP photocathodes

Cite as: Appl. Phys. Lett. **128**, 083501 (2026); doi: 10.1063/5.0315264
Submitted: 4 December 2025 · Accepted: 10 February 2026 ·
Published Online: 24 February 2026

Adam Masters,[1] Greg Blume,[1] Sushil Poudel,[1] Joseph Michael Grames,[2] Matt Poelker,[2] Marcy Stutzman,[2] Stephen Polly,[3] Seth M. Hubbard,[3] Sylvain Marsillac,[1] and Matt Grau[1,a)]

AFFILIATIONS

[1]Old Dominion University, 5115 Hampton Blvd, Norfolk, Virginia 23529, USA
[2]Thomas Jefferson National Accelerator Facility, 12000 Jefferson Avenue, Newport News, Virginia 23606, USA
[3]Rochester Institute of Technology, 1 Lomb Memorial Drive, Rochester, New York 14623, USA

[a)]**Author to whom correspondence should be addressed:** mgrau@odu.edu

ABSTRACT

Strained superlattice GaAs photocathodes are crucial for providing high photocurrent beams of spin-polarized electrons at several accelerator facilities including the Continuous Electron Beam Accelerator Facility at Thomas Jefferson National Accelerator Facility and the future Electron–Ion Collider at Brookhaven National Laboratory. In this work, we study the effects of varying the number of superlattice pairs on the polarization and photocurrent of the photocathodes. We observe a saturation in quantum efficiency beyond 30 pairs, with additional layers yielding minimal photocurrent improvement while noticeably reducing the polarization of the beam.

The need to improve polarized electron sources beyond their current capabilities has become increasingly important as accelerator facilities continue to advance their studies of fundamental physics. The Electron–Ion Collider (EIC) requires 7 nC of bunch charge with 85% spin polarization,[1] while the Continuous Electron Beam Accelerator Facility (CEBAF) requires 1% quantum efficiency (QE) and polarization above 85%,[2] and higher quantum efficiency above is needed to generate spin-polarized positron beams.[3,4]

In unstrained bulk GaAs, the heavy-hole (HH) and light-hole (LH) valence bands are degenerate at the Γ point. Circularly polarized light at the band edge excites electrons from both bands with opposite spin orientations, and the transition matrix elements favor HH excitation by a factor of three. This limits the theoretical maximum electron spin polarization to 50%.[5] To do any better than this limit, the HH–LH degeneracy must be lifted so that optical excitation near the bandgap excites electrons predominantly from a single valence band. Biaxial compressive strain lifts this degeneracy by shifting the HH band to higher energy.[6] In GaAs/GaAsP heterostructures, the lattice constant of GaAs exceeds that of GaAsP, so thin GaAs layers grown on GaAsP experience in-plane compression. With sufficient HH–LH splitting, circularly polarized photons tuned to the HH transition excite electrons of a single spin orientation, enabling polarization approaching 100%.[7]

In a strained superlattice, alternating layers of GaAs and GaAsP allow the strain to be maintained across many periods without relaxation. A single thick strained layer would exceed the critical thickness and relax, degrading polarization. By using many thin strained layers, the optical depth of the material increases while each layer remains coherently strained, improving both QE and polarization simultaneously.[8]

Strained superlattice photocathodes have traditionally been grown using molecular beam epitaxy (MBE).[8] Metal-organic chemical vapor deposition (MOCVD)-grown photocathodes are an alternative and have demonstrated comparable polarization to MBE-grown devices while reaching quantum efficiency above 2%.[1,9] In 2004, Maruyama *et al.* from the Stanford Linear Accelerator Center performed a study varying the number of superlattice pairs that were lattice matched to the virtual substrate in MBE grown photocathodes.[10] This study showed that past 15 pairs, the maximum polarization of the beam extracted from the photocathode decreased significantly. As a result, most photocathodes grown after this time have incorporated a superlattice comprising fewer than 15 pairs. Recent studies at Brookhaven National Laboratory (BNL) have demonstrated spin polarization of 62% and QE of 15.5% in a strained superlattice device grown by MBE containing as many as 30 pairs, in a superlattice that is strain compensated to the virtual substrate.[11] In this study, we focus on using strained superlattice grown by MOCVD and studying the

effect of the number of pairs of superlattice on both polarization and quantum efficiency.

Strained GaAs grown on GaAsP virtual substrates were shown to improve spin polarization of photocathodes beyond the capability of bulk GaAs.[8] By incorporating quantum well structures using alternating GaAs/GaAsP layers, polarization and quantum efficiency were further enhanced. While state-of-the-art photocathodes contain a distributed Bragg reflector (DBR) to enhance QE of the device, in this study we opted to focus only on the effects of the superlattice itself, to avoid any effects of potential strain due to lattice mismatch in the DBR layers relative to the virtual substrate and superlattice from affecting the results.[12] We grew all devices using an AIXTRON close-coupled showerhead MOCVD system. The wafers used were zinc-doped (100) on-axis GaAs substrates. We grew a metamorphic graded composition from GaAs to $GaAs_{0.65}P_{0.35}$ in 2.5% increments of phosphorus, each 500 nm thick. We grew a 500 nm overshoot layer of $GaAs_{0.625}P_{0.375}$ followed by a 2750 nm $GaAs_{0.65}P_{0.35}$ buffer layer. The superlattice structure on top of this virtual substrate consisted of alternating layers of 3.8 nm thick GaAs and 2.8 nm thick layers of GaAsP with an intended composition of $GaAs_{0.65}P_{0.35}$. We refer to the GaAs layers of the superlattice as wells and the GaAsP layers as barriers due to their relative bandgap. We based all composition and thickness growth targets on previously established compositions measured using high-resolution x-ray diffraction (HRXRD) reciprocal space maps and *in situ* telemetry. The number of pairs of (GaAs/GaAsP) in the superlattice varied between 14 and 46. The final layer grown was a 5 nm GaAs p-type layer, carbon-doped at 5×10^{19} cm^{-3},[13] which facilitates the band bending necessary to extract the electrons from the device when activated with cesium and nitrogen trifluoride and prevent surface charging effect.[14]

To ensure proper lattice relaxation within the metamorphic grading, the buffer layers were analyzed after deposition at room temperature via high resolution x-ray diffraction techniques using a Bruker D8 Discover system. In particular, asymmetrical (224) glancing exit reciprocal space maps were used. We observed the metamorphic graded layers to be fully relaxed, with phosphorus composition close to the targeted value of 35%. Nomarski microscopy images indicated that these growths led to smooth and uniform surfaces.

The crystal quality of the superlattice layers in the various devices was evaluated by transmission electron microscopy (TEM) using a Thermo-Fisher Titan 80-300 Aberration Corrected STEM system. We observed all superlattice layers to be uniform with abrupt junctions on the order of one to two atomic layers, regardless of the number of pairs (Fig. 1). Any vertical lines appearing in the images are TEM sample preparation artifacts, namely curtain effects that are caused by small thickness variations in the sample as a result of the focused ion beam method used to extract the superlattice from the wafer. The thicknesses of both GaAs and GaAsP layers appear to be uniform from the bottom to the top of the structure (Fig. 2), with values close to the targeted values of 3.8 nm for GaAs (brighter layer) and 2.8 nm for GaAsP (darker layer). The composition of each layer was checked using HRXRD and energy dispersive x-ray spectroscopy (EDS) associated with the TEM system (Fig. 2). The composition of the 2750 nm $GaAs_{0.65}P_{0.35}$ buffer layer was confirmed by HRXRD. We observe a modest systematic offset in the EDS measurements (Fig. 2), where for $GaAs_{0.65}P_{0.35}$ we measure an atomic composition of 38% arsenic and 12% phosphorous, when we would expect 32.5% and 17.5%, respectively, due to the lack of a calibration sample. However, we still note a uniform composition across all 14 layers of the superlattice. The fact that the EDS map is not as sharp as the TEM imaging is due in part to the nature of the EDS measurement, resulting in a cone-shaped emission volume.

Following the fabrication in the MOCVD system, each sample was removed and N_2 bagged for transport. During this process, the samples were temporarily exposed to atmosphere, which allowed surface contamination to form on the surface. To counteract this contamination, the samples were first HCl etched for 30 s prior to installation. Following installation, the samples were heated to a surface temperature of 550 °C to remove any further oxidation and prepare for activation. Each sample was activated using the "Yo-Yo" technique using a SAES cesium getter and NF_3 until the relative photocurrent gain was less than 5%. The behavior of all the photocathodes during activation was uniform. The preparation of a photocathode strongly influences its electron affinity, and therefore its QE.[15] We assume that, since all the samples referenced here were fabricated, prepared, and activated in the same manner, they have similar effective electron affinity. Immediately following the activation, the QE and polarization were

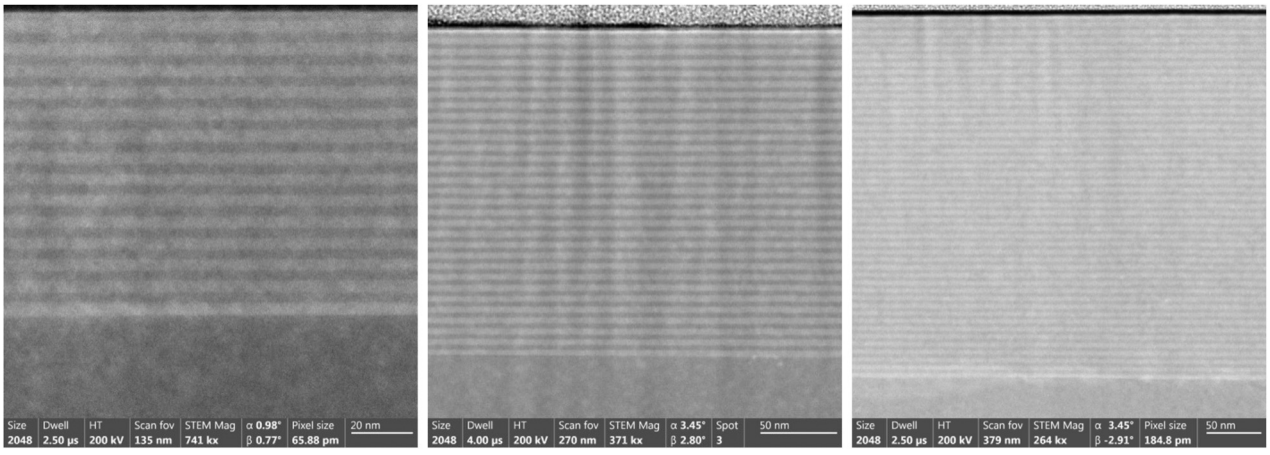

FIG. 1. STEM images of the 14, 30, and 46 pair superlattices at magnifications of 741k×, 371k×, and 264k×, respectively.

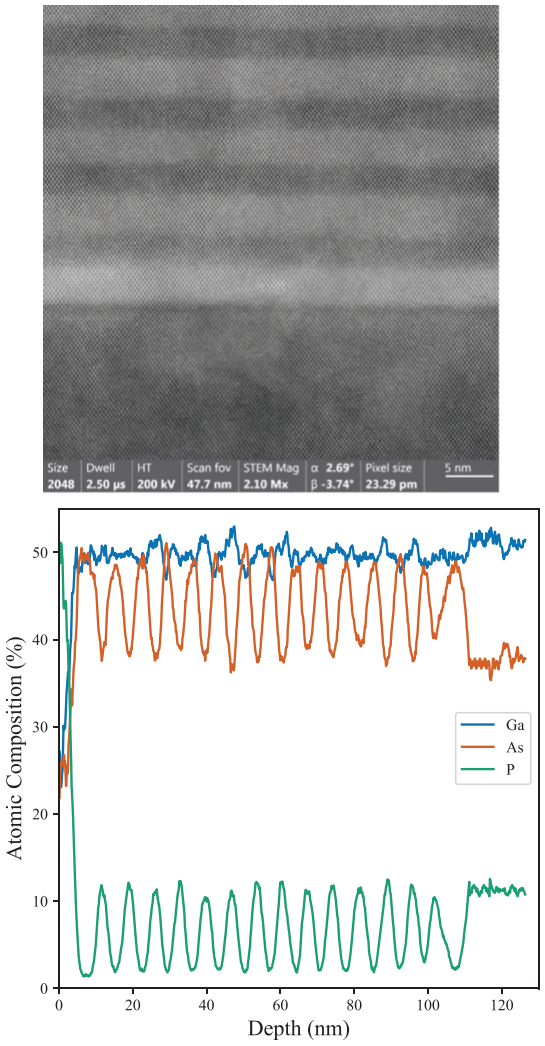

FIG. 2. Left: STEM image of the 14 pair superlattice (magnification of 2.1M×; scale bar: 5 nm). Right: EDS line map of the 14 pair superlattice indicating Ga, As, and P atomic composition.

evaluated using a microMott polarimeter at the Thomas Jefferson National Accelerator Facility.[16] We bias the activated sample to −248 V and illuminate it at normal incidence with a focused beam of circularly polarized light from a tunable wavelength laser. We can choose to use either left or right handed polarized light by inserting a half wave plate into the beam path prior to a zero-order quarter wave plate. The angle of the waveplates is set to maximize the polarization to near 100% at 780 nm, and due to the variation in retardation with wavelength the degree of circular polarization varies by 2% over the 110 nm wavelength range over which we characterize the photocathodes. The incident light generates longitudinal spin-polarized photoelectrons that are then deflected 90° and electrostatically steered toward a gold target biased at +20 kV. This bias voltage accelerates the electrons to an energy of 20 keV where the now transversely spin-polarized electrons scatter asymmetrically via Mott scattering.[17] These scattered electrons are decelerated by 20 kV, then counted in detectors placed at angles corresponding to the maximum of the Sherman function, the spin asymmetry analyzing power in elastic electron scattering. We use retarding field grids placed in front of the detectors, variably biased from 150 to 320 V to isolate elastically scattered electrons. We repeat this measurement process for each wavelength of incident light.

We found that increasing the number of superlattice pairs up to 30 pairs led to an expected increase in the quantum efficiency at 780 nm excitation, at which point we observe minimal gains with additional pairs (Fig. 3 top). This is likely due to carrier recombination in the superlattice.[18] Polarization at the peak wavelength was above 89% for photocathodes with up to 30 pairs. With more superlattice pairs, the polarization tends to decrease (Fig. 3 bottom), likely due to depolarization of electrons emitted further from the surface.[18]

One of the trends observed in Fig. 3 is the wavelength shift of the maximum polarization as a function of the number of pairs, with a value ranging from 90.1% at 785 nm for 14 pairs to 84.1% at 800 nm for 46 pairs. Generally, this type of trend comes from either sample-to-sample disparity of the composition, spatial non-uniformity of the composition, or strain relaxation. The composition for each pair was checked by HRXRD and EDS and no obvious trend was observed. We then used a Horiba iHR320 Photoluminescence (PL) spectrometer to measure the photoemission of the superlattice pairs when irradiated by a 532 nm laser light. We acquired PL mapping of the wafer surface on the various samples to gain insight into potential spatial non-uniformity within a sample. PL mapping showed a high surface uniformity for each sample. The last characterization consisted in looking at PL intensity values from the center of the samples for wavelength in the 770–810 nm range, corresponding nominally to the strained GaAs peak (Fig. 4). As one can see, the peak position shifts from 782 nm for 14 pairs to 797 nm for 46 pairs. The change in the maximum polarization is therefore consistent with a shift of the strained GaAs peak, as observed by PL. Since this shift in the peak position does not seem to come predominantly from a shift of the GaAsP composition across samples, it is likely due to an increase in strain relaxation that occurs as more pairs of superlattice are fabricated. A strain relaxation dependent shift is supported by the photoluminescence peak in the strained 14 pair superlattice being close in value to the one calculated based on $GaAs_{0.6}P_{0.35}$ buffer layer (780 nm), and then relaxing back toward higher wavelength as the number of pairs increases and the strain relaxes. Looking back at the quantum efficiency (Fig. 3), one can see a clear shift in the onset of absorption, from approximately 784 nm for the 14 pair sample to 802 nm for the 38 and 46 pair sample, consistent with a shift in the GaAs peak. This relaxation in the strain for higher number of pairs is also consistent with a decrease in the polarization with higher number of pairs.

In this study, we tested the effects of varying the number of superlattice pairs in photocathodes grown via the MOCVD process using compressive superlattice barriers. Transmission electron microscopy and high-resolution x-ray diffraction show that the devices maintained high crystal quality in the superlattice and are close to the targeted composition. Data collected from photoluminescence indicate that devices exhibit high uniformity across the surface and that peak emission tends toward higher excitation wavelengths as the number of superlattice pairs increases. Device measurements show that increasing the number of pairs beyond 30 pairs degrades polarization while only increasing QE minimally. Polarization data indicate all devices are

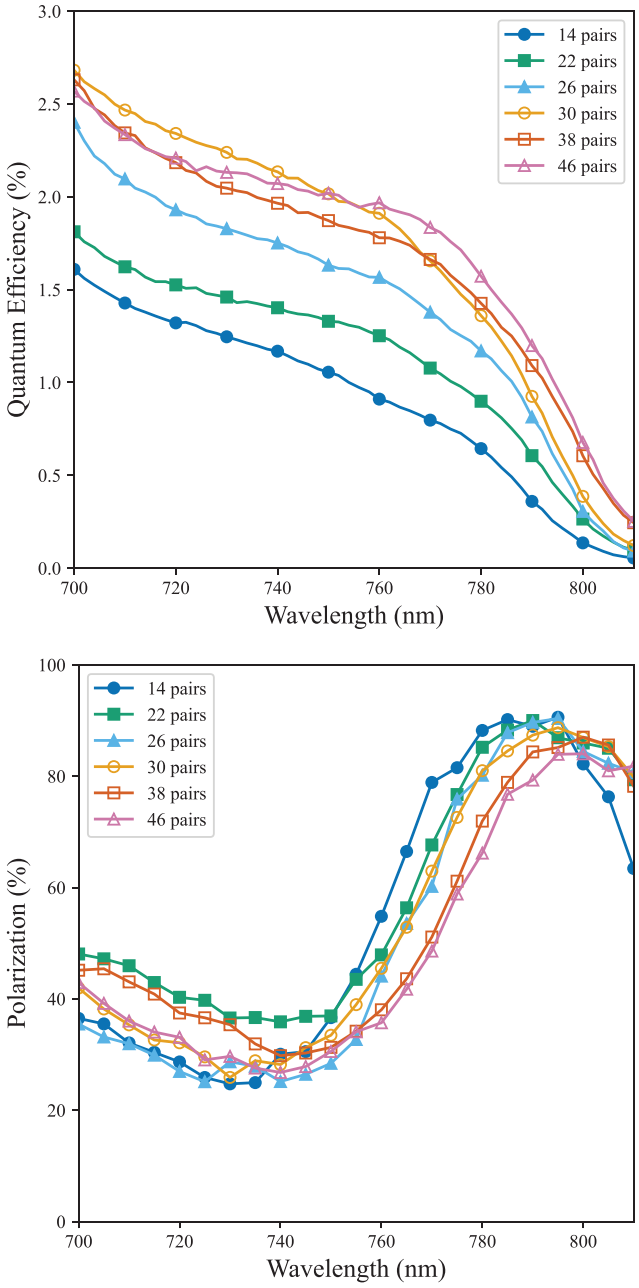

FIG. 3. (Top) Measured quantum efficiency of each device as a function of wavelength. (Bottom) Measured polarization of each device as a function of wavelength. Relative measurement uncertainties for the quantum efficiency are 5% and statistical measurement uncertainties for polarization are reported as 2 σ error bars.

capable of more than 84% polarization at their bandgap photon energies with values of 89% polarization and 1.4% QE for the 30 pairs devices at 780 nm. The ability to increase the number of pairs in the superlattice from 15 pairs[10] to 30 pairs in this study is a testimony to the enhancement of both the deposition system and the understanding of growth processes for the past 20 years.[19,20] The fact that we used an

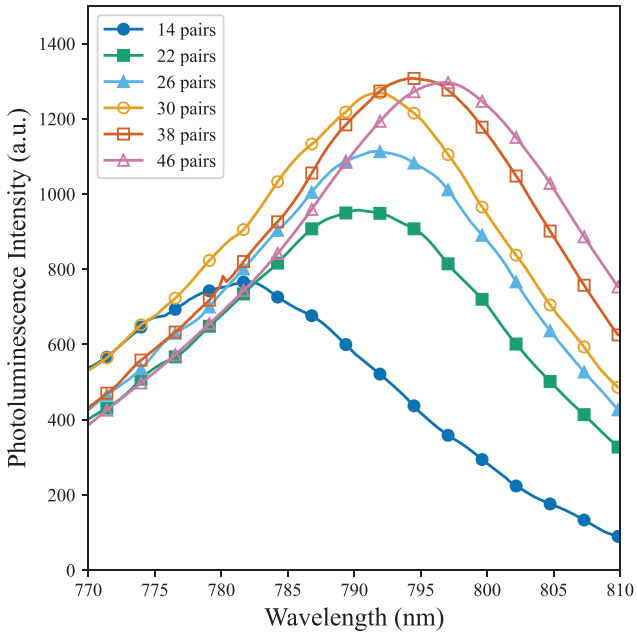

FIG. 4. Photoluminescence intensity measured at the center of each of the six devices as a function of wavelength.

MOCVD system instead of an MBE system might be a contributing factor, as both systems have specific advantages,[21] but MBE systems have themselves made tremendous progress in 20 years[22,23] and are expected to get the same results.

This material is based upon work supported by the U.S. Department of Energy, Office of Nuclear Physics, Contract No. DE-SC0023369. This work was performed in part at the Analytical Instrumentation Facility (AIF) at North Carolina State University, which is supported by the State of North Carolina and the National Science Foundation (Award No. ECCS-2025064). The AIF is a member of the North Carolina Research Triangle Nanotechnology Network (RTNN), a site in the National Nanotechnology Coordinated Infrastructure (NNCI).

AUTHOR DECLARATIONS

Conflict of Interest

The authors have no conflicts to disclose.

Author Contributions

Adam Masters: Conceptualization (equal); Formal analysis (equal); Investigation (equal); Writing – original draft (equal). **Greg Blume:** Formal analysis (equal); Investigation (equal); Writing – review & editing (equal). **Sushil Poudel:** Investigation (equal); Writing – review & editing (equal). **Joseph Michael Grames:** Formal analysis (equal); Funding acquisition (equal); Investigation (equal); Writing – review & editing (equal). **Matt Poelker:** Writing – review & editing (supporting). **Marcy Stutzman:** Writing – review & editing (supporting). **Stephen Polly:** Investigation (equal); Writing – review & editing

(equal). **Seth M. Hubbard:** Investigation (equal); Writing – review & editing (equal). **Sylvain Marsillac:** Conceptualization (equal); Formal analysis (equal); Funding acquisition (equal); Project administration (equal); Supervision (equal); Writing – original draft (equal). **Matt Grau:** Conceptualization (equal); Formal analysis (equal); Funding acquisition (equal); Project administration (equal); Supervision (equal); Writing – original draft (equal).

DATA AVAILABILITY

The data that support the findings of this study are available from the corresponding author upon reasonable request.

REFERENCES

[1]J. Biswas, E. Wang, J. Skaritka, O. Rahman, K. Kisslinger, T.-D. Li, A. Masters, and S. Marsillac, in JACoW IPAC2024, MOPR77, 2024.
[2]J. Grames and M. Poelker, "Polarized electron sources," in *Polarized Beam Dynamics and Instrumentation in Particle Accelerators: USPAS Summer 2021 Spin Class Lectures*, edited by F. Méot, H. Huang, V. Ptitsyn, and F. Lin (Springer International Publishing, Cham, 2023), pp. 261–284.
[3]J. Grames, J. Benesch, M. Bruker, L. Cardman, S. Covrig, P. Ghoshal, S. Gopinath, J. Gubeli, S. Habet, C. Hernandez-Garcia, A. Hofler, R. Kazimi, F. Lin, S. Nagaitsev, M. Poelker, B. Rimmer, Y. Roblin, V. Lizarraga-Rubio, A. Seryi, M. Spata, A. Sy, D. Turner, A. Ushakov, C. A. Valerio-Lizarraga, and E. Voutier, "Positron beams at Ce^{+}BAF," arXiv:2309.15581 [physics.acc-ph] (2023).
[4]E. Voutier, in *EPJ Web of Conferences* (EDP Sciences, 2024), Vol. 303, p. 06003.
[5]D. T. Pierce and F. Meier, Phys. Rev. B **13**, 5484 (1976).
[6]T. Maruyama, E. L. Garwin, R. Prepost, and G. H. Zapalac, Phys. Rev. B **46**, 4261 (1992).
[7]T. Maruyama *et al.*, Appl. Phys. Lett. **85**, 2640 (2004).
[8]W. Liu, Y. Chen, W. Lu, A. Moy, M. Poelker, M. Stutzman, and S. Zhang, Appl. Phys. Lett. **109**, 252104 (2016).
[9]B. Belfore, A. Masters, D. Poudel, G. Blume, S. Polly, E. Wang, S. M. Hubbard, M. Stutzman, J. M. Grames, M. Poelker, M. Grau, and S. Marsillac, Appl. Phys. Lett. **123**, 222102 (2023).
[10]T. Maruyama, D. Luh, A. Brachmann, J. E. Clendenin, E. L. Garwin, S. Harvey, J. Jiang, R. E. Kirby, C. Y. Prescott, R. Prepost, and A. M. Moy, in *SPIN 2004*, edited by F. Bradamante, A. Bressan, A. Martin, and K. Aulenbacher (World Scientific, 2005), pp. 917–921.
[11]J. Biswas, L. Cultrera, W. Liu, E. Wang, J. Skaritka, K. Kisslinger, S. D. Hawkins, S. R. Lee, and J. F. Klem, AIP Adv. **13**, 085106 (2023).
[12]T. Nakanishi, H. Aoyagi, H. Horinaka, Y. Kamiya, T. Kato, S. Nakamura, T. Saka, and M. Tsubata, Phys. Lett. A **158**, 345 (1991).
[13]S. A. Stockman, G. E. Höfler, J. N. Baillargeon, K. C. Hsieh, K. Y. Cheng, and G. E. Stillman, J. Appl. Phys. **72**, 981 (1992).
[14]T. Maruyama, A. Brachmann, J. Clendenin, T. Desikan, E. Garwin, R. Kirby, D.-A. Luh, J. Turner, and R. Prepost, Nucl. Instrum. Methods Phys. Res., Sect. A **492**, 199 (2002).
[15]L. B. Jones, M. F. Sherwin, G. R. Bell, P. M. Sherwin, L. F. Sherwin *et al.*, J. Phys. D **54**, 205301 (2021).
[16]J. McCarter, M. Stutzman, K. Trantham, T. Anderson, A. Cook, and T. Gay, Nucl. Instrum. Methods Phys. Res., Sect. A **618**, 30 (2010).
[17]G. Blume, M. Bruker, C. Cuevas, H. Dong, B. Fernandes Neres, P. Ghoshal, S. Gopinath, J. Grames, S. Gregory, G. Hays, C. L. Galliard, S. Marsillac, B. Moffit, T. Nguyen Trung, M. Poelker, R. Suleiman, E. Voutier, and S. Zhang, Nucl. Instrum. Methods Phys. Res., Sect. A **1062**, 169224 (2024).
[18]W. Liu, M. Poelker, X. Peng, S. Zhang, and M. Stutzman, J. Appl. Phys. **122**, 035703 (2017).
[19]R. Dupuis, J. Vac. Sci. Technol., B **41**, 060803 (2023).
[20]X. Zhang, N. Trainor, T. V. Mc Knight, A. R. Graves, Z. Wu, L. Xu, X. Zheng, T. Zhang, J. Zhu, T. Palacios, J. Kong, B. Groven, B. Tian, C. Duan, J. Chu, and J. M. Redwing, Nat. Rev. Methods Primers **5**, 57 (2025).
[21]A. L. B. Price, "Embedded HSQ nanostructures in GaAs homoepitaxy by MOCVD and MBE: A study of selective area epitaxy at the nanoscale," Master's thesis (Ohio State University, 2024).
[22]W. Hidayat and M. Usman, Phys. Scr. **99**, 112002 (2024).
[23]R. Choudhary and B. Jalan, Device **3**, 100711 (2025).